

Production of Oxaporphyrin and Biliverdin Derivatives by Coupled Oxidation of Cobalt(II) Octaethylporphyrin

Alan L. Balch,* Marinella Mazzanti, Tamara N. St. Claire, and Marilyn M. Olmstead

Department of Chemistry, University of California, Davis, California 95616

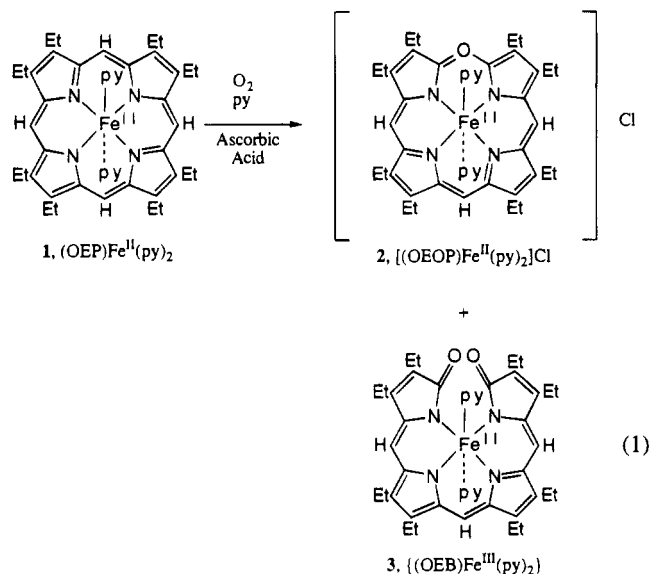
Received November 4, 1994[⊗]

The ability of cobalt, rather than iron, to participate in the oxidative cleavage of porphyrins, a reaction related to that of the enzyme heme oxygenase, has been explored. Treatment of (octaethylporphyrin)cobalt(II) with dioxygen in the presence of ascorbic acid, as a reducing agent, in dichloromethane/tetrahydrofuran produces a green solution that can yield the cobalt verdoheme analogs $\{(\text{OEOP})\text{Co}^{\text{II}}(\text{PF}_6)\}$ and $\{(\text{OEOP})\text{Co}^{\text{III}}\text{Cl}_2\}$ (OEOP is the monoanion of octaethyloxaporphyrin), $\{(\text{OEB})\text{Co}\}$, a complex of the open chain tetrapyrrole octaethylbilindione (H_3OEB), or octaethylbilindione itself. These products have been isolated and characterized by uv/vis and ^1H NMR spectroscopy. $\{(\text{OEOP})\text{Co}^{\text{II}}(\text{PF}_6)\}\cdot\text{CH}_2\text{Cl}_2$ ($\text{C}_{36}\text{H}_{45}\text{Cl}_2\text{CoF}_6\text{N}_6\text{N}_4\text{OP}$) crystallizes in the triclinic space group $P\bar{1}$, with $a = 11.077(2)$ Å, $b = 14.033(2)$ Å, $c = 14.099(3)$ Å, $\alpha = 104.56(2)^\circ$, $\beta = 101.70(2)^\circ$, and $\gamma = 110.70(1)^\circ$ at 130 K with $Z = 2$. Refinement of 4171 reflections with $F > 4.0\sigma(F)$ and 450 parameters yielded $R = 0.066$; $R_w = 0.060$. The structure of the complex cation consists of a flat macrocycle with planar, four-coordinate cobalt at the center. These cations associate in π - π fashion with a mean-plane separation of 3.261 Å and a short lateral displacement of 1.506 Å. $\{(\text{OEOP})\text{Co}^{\text{III}}\text{Cl}_2\}\cdot 2\text{CH}_2\text{Cl}_2$ ($\text{C}_{37}\text{H}_{47}\text{Cl}_6\text{CoN}_4\text{O}$) crystallizes in the monoclinic space group $P2_1/c$, with $a = 12.702(5)$ Å, $b = 8.125(3)$ Å, $c = 19.327(5)$ Å, and $\beta = 101.23(2)^\circ$ at 130 K with $Z = 2$. Refinement of 1803 reflections with $F > 4.0\sigma(F)$ and 218 parameters yielded $R = 0.057$; $R_w = 0.054$. The structure of the centrosymmetric complex consists of a six-coordinate cobalt ion with two axial chloride ligands and a planar oxaporphyrin which is disordered with regard to the location of the peripheral oxygen atom.

Introduction

Treatment of iron(II) porphyrins with dioxygen in the presence of a reducing agent such as ascorbic acid or hydrazine in pyridine (py) produces a deep green solution that has been known since 1930 to contain a diamagnetic iron complex, verdoheme.^{1–5} This is illustrated in eq 1 for the symmetrical series that is derived from octaethylporphyrin (OEPH₂). While several structures have been suggested for verdoheme, it has recently been possible to crystallize some verdoheme analogs and firmly establish the presence of the planar oxaporphyrin ligand (OEOP)[−] in these complexes.⁶ Verdoheme formation accounts for only about 50% of the heme that is lost by this oxidation. A major portion of the remaining material has been shown to be the paramagnetic biliverdin-type complex, $\{(\text{OEB})\text{Fe}^{\text{III}}(\text{py})_2\}$.⁷ The oxidation of heme in this coupled oxidation process has been widely adopted as a model for the catabolism of heme that is accomplished by heme oxygenase.⁸

The metal ion that is present within the porphyrin has a key role in activating dioxygen and facilitating its attack on the



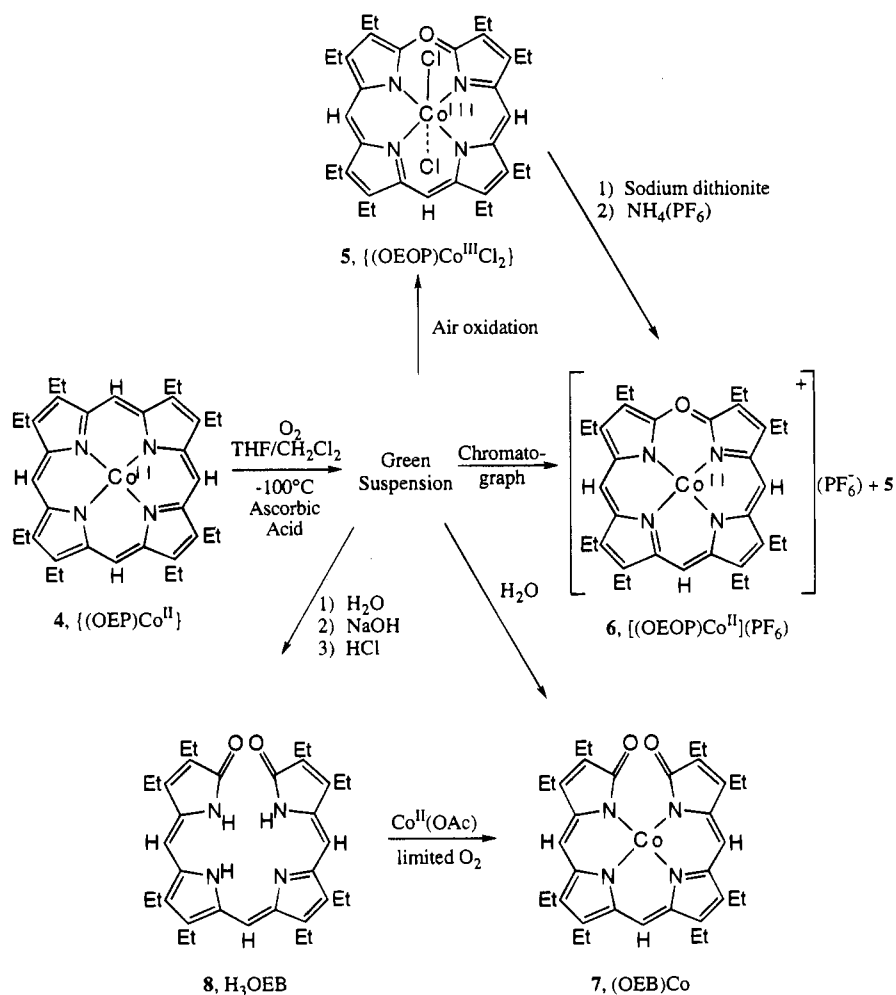
[⊗] Abstract published in *Advance ACS Abstracts*, March 1, 1995.

- (1) Warburg, O.; Negelein, E. *Chem. Ber.* **1930**, *63*, 1816.
- (2) O'Carra, P. In *Porphyrins and Metalloporphyrins*; Smith K. M., Ed.; Elsevier: New York, 1975; p 123.
- (3) Schmid, R.; McDonagh, A. F. In *The Porphyrins*; Dolphin, D., Ed.; Academic Press: New York, 1979; Vol. 6, p 258.
- (4) Brown, S. B. In *Bilirubin*; Heirwegh, K. P. M., Brown, S. B., Eds.; CRC Press, Inc.: Boca Raton, FL, 1982; Vol. 2, p 1.
- (5) Bissell, D. M. in *Liver: Normal Function and Disease. Volume 4. Bile Pigments and Jaundice*; Ostrow, J. D., Ed.; Marcel Dekker, Inc.: New York, 1986; p 133.
- (6) Balch, A. L.; Latos-Grażyński, L.; Noll, B. C.; Olmstead, M. M.; Sztrenberg, L.; Safari, N. *J. Am. Chem. Soc.* **1993**, *115*, 1422. Balch, A. L.; Koerner, R.; Olmstead, M. M. *J. Chem. Soc., Chem. Commun.*, in press.
- (7) Balch, A. L.; Latos-Grażyński, L.; Noll, B. C.; Olmstead, M. M.; Safari, N. *J. Am. Chem. Soc.* **1993**, *115*, 9056.
- (8) Maines, M. D. *Heme Oxygenase: Clinical Applications and Functions*. CRC Press: Boca Raton, FL, 1992.

porphyrin periphery, both in the enzymatic reaction and in the model coupled oxidation process. Protoporphyrin IX itself is not oxidized by heme oxygenase and some metalloporphyrins; tin(IV) and zinc(II) heme for example, act as inhibitors of the enzyme.⁹ Cobalt(II) porphyrins, like iron(II) porphyrins, are capable of reversible dioxygen binding^{10,11} and might be expected to participate in the essential activation process that initiates porphyrin degradation. There was an initial report that cobalt(II) heme was oxidized by heme oxygenase,¹² but more

- (9) Drummond, G. S.; Kuppas, A. *Proc. Natl. Acad. Sci. U.S.A.* **1981**, *78*, 6466.
- (10) Walker, F. A. *J. Am. Chem. Soc.* **1970**, *92*, 4235.
- (11) Basolo, F.; Hoffman, B. M.; Ibers, J. A. *Acc. Chem. Res.* **1975**, *8*, 384.
- (12) Maines, M. D.; Kappas, A. *Biochemistry* **1977**, *16*, 419.

Scheme 1

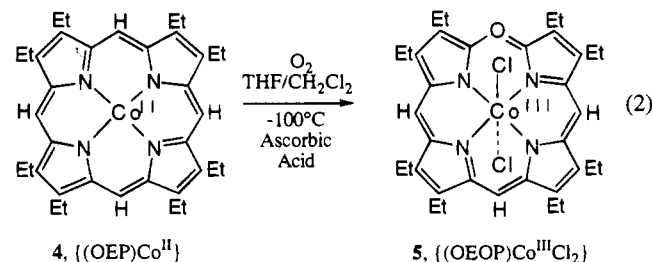


recent results have concluded that no enzymatic oxidation of cobalt heme occurs.^{13,14} Myoglobin and hemoglobin that are reconstituted with cobalt(II) heme do form biliverdin when exposed to dioxygen and ascorbate.¹⁵ In pyridine solution under typical coupled oxidation conditions that are used for iron porphyrins, cobalt(II) porphyrins are merely converted to cobalt(III) porphyrins without the formation of either a cobalt analog of verdoheme or of a complex of biliverdin.^{14–16} We recently reported that it was possible to find conditions that did allow the conversion of cobalt(II) octaethylporphyrin into a verdoheme analog—cobalt(III) octaethylloxaporphyrin dichloride, **5**—as shown in eq 2.¹⁶ The use of a poorly coordinating solvent mixture—

this reaction and describe the isolation of other cobalt complexes that are formed in this modified coupled oxidation.

Results

Synthetic Studies. Addition of dioxygen to a partially frozen mixture of $\{(OEP)Co^{II}\}$ and ascorbic acid in a mixture of dichloromethane–THF (8:1 v/v) followed by warming to room temperature produces a green suspension which can yield three different cobalt complexes or the open tetrapyrrole, octaethylbilindione, H_3OEB , **8**. The interrelationships of these products are shown in Scheme 1. In each work up the green suspension is filtered to remove excess ascorbic acid. If the reaction mixture is made dioxygen free, then purple $[(OEOP)Co^{II}](PF_6)$ is obtained after chromatography and treatment with ammonium hexafluorophosphate in 48% yield. This procedure also gives a 21% yield of burgundy $\{(OEOP)Co^{III}Cl_2\}$. If the green solution is allowed to stir in air for 24 h, the cobalt(II) complex is oxidized and $\{(OEOP)Co^{III}Cl_2\}$ can be obtained as the major product with a 62% yield. $\{(OEOP)Co^{III}Cl_2\}$ is reduced by aqueous sodium dithionite and in the presence of ammonium hexafluorophosphate forms $[(OEOP)Co^{II}](PF_6)$. When the original green solution is washed with water and subjected to chromatography, a 24% yield of olive-green $\{(OEB)Co\}$ results. When the green solution is treated successively with water, sodium hydroxide and hydrochloric acid a 50% yield of the linear tetrapyrrole H_3OEB , **8**, is formed. Treatment of H_3OEB with cobalt(II) acetate in air followed by recrystallization under a dinitrogen atmosphere yields $\{(OEB)Co\}$, **7**. This olive green complex has been previously prepared by the addition of cobalt-



dichloromethane and tetrahydrofuran (THF)—is crucial to the success of this process. Here we report on further details of

- (13) Yoshida, T.; Kikuchi, G. *J. Biol. Chem.* **1978**, *253*, 8479.
 (14) King, R. F. G. J.; Brown, S. B. *Biochem. J.* **1978**, *174*, 103.
 (15) Vernon, D. I.; Brown, S. B. *Biochem. J.* **1984**, *223*, 205.
 (16) Balch, A. L.; Mazzanti, M.; Olmstead, M. M. *J. Chem. Soc., Chem. Commun.* **1994**, 269.

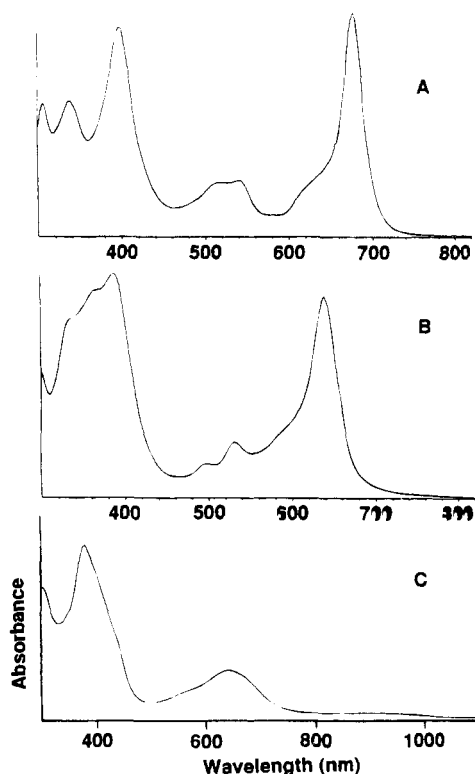


Figure 1. Electronic absorption spectra [λ_{max} , nm (ϵ , $\text{cm}^{-1} \text{M}^{-1}$)] of chloroform solutions: (A, $\{(\text{OEOP})\text{Co}^{\text{III}}\text{Cl}_2\}$) 338 (5.3×10^4), 398 (8.2×10^4), 514 (2.0×10^4), 540 (2.1×10^4), 620 sh (1.8×10^4), 678 (8.8×10^4); (B, $\{(\text{OEOP})\text{Co}^{\text{II}}(\text{PF}_6)\}$) 332 (3.7×10^4), 364 (4.3×10^4), 388 (4.6×10^4), 496 (1.0×10^4), 532 (1.4×10^4), 584 sh (1.6×10^4), 640 (4.2×10^4); (C, $\{(\text{OEB})\text{Co}\}$) 380 (6.7×10^4), 642 (1.9×10^4).

(I) acetate to H_3OEB and thoroughly characterized.^{17,18} It contains a four-coordinate and approximately planar cobalt center which is coordinated by the helical tetrapyrrole through its four nitrogen atoms.

The three cobalt complexes, **5**, **6**, and **7**, are readily distinguished by their electronic absorption spectra which are shown in Figure 1. The spectra of **5** and **6** with strong absorption in the 650–700 nm region are typical of those of complexes that contain the oxaporphyrin ligand. They closely resemble the spectrum of octaethylverdoheme.¹⁶ In contrast, the spectrum of **7**, $\{(\text{OEB})\text{Co}\}$ consists of a set of broad peaks at ca 400 and 540 nm.

The complexes are also readily identified by their ^1H NMR spectra. The spectrum of $\{(\text{OEOP})\text{Co}^{\text{III}}\text{Cl}_2\}$ is that of a typical diamagnetic complex with two meso resonances at 9.71 and 9.70 ppm, four methyl triplets in the 1.7–1.9 ppm region, and a complex multiplet of methylene resonances at 3.68 ppm. Details are given in the experimental section. The ^1H NMR spectrum of $\{(\text{OEOP})\text{Co}^{\text{II}}(\text{PF}_6)\}$ is shown in Figure 2. The spectral pattern resembles that of $(\text{OEP})\text{Co}^{\text{II}}$, which has a meso proton resonance at 29.4 ppm, a methylene resonance at 8.8 ppm, and a methyl resonance at 6.1 ppm in chloroform-*d* solution at 26 °C. The spectrum of $\{(\text{OEOP})\text{Co}^{\text{II}}(\text{PF}_6)\}$ has been assigned on the basis of the observed relative intensities (obtained under normal, not inversion recovery, conditions) and linewidths. There are two meso resonances with marked downfield hyperfine shifts (at 17.1 and 23.7 ppm). The methyl groups produce three, relatively narrow resonances. The one

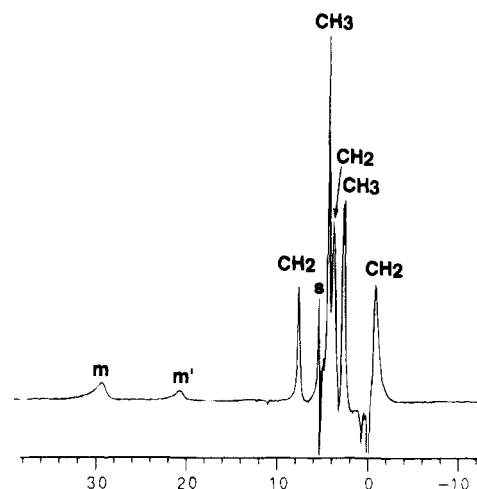


Figure 2. ^1H NMR spectrum of $\{(\text{OEOP})\text{Co}^{\text{II}}(\text{PF}_6)\}$ at 23 °C in dichloromethane- d_2 . The spectrum was taken under inversion recovery so that the peaks due to diamagnetic materials are largely inverted. Resonance assignments are as follows: m and m', meso protons; CH₃, methyl protons; CH₂, methylene protons; s, solvent.

at 5 ppm has twice the intensity of the other two. Three, relatively broader resonances are assigned to the methylene protons. The ^1H NMR spectral data for $\{(\text{OEB})\text{Co}\}$ are discussed in detail in ref 17.

In solution at 25 °C the magnetic moment of $\{(\text{OEOP})\text{Co}^{\text{II}}(\text{PF}_6)\}$ is $1.9(3) \mu_{\text{B}}$. In the solid state the magnetic moment is $2.04(6) \mu_{\text{B}}$ at 8 °C.

Crystal and Molecular Structure of $\{(\text{OEOP})\text{Co}^{\text{II}}(\text{PF}_6)\} \cdot \text{CH}_2\text{Cl}_2$. The results of an X-ray diffraction study are given in Tables 1 and 2, which contain the atomic coordinates and a listing of selected interatomic distances and angles, respectively. The compound consists of the cation, a molecule of dichloromethane, and a hexafluorophosphate ion which is orientationally disordered so that there are two sets of fluorine atom positions.

A view of the complex cation is shown in Figure 3. The cobalt(II) ion is four coordinate and planar. The average Co–N distance is 1.944(3) Å. This is similar to the Co–N distance (1.949(3) Å) in $(\text{TPP})\text{Co}^{\text{II}}$ (TPP is the dianion of *meso*-tetraphenylporphyrin) which has a ruffled porphyrin core.²⁰ In related planar porphyrins, *meso*-(tetrakis(tetrafluoro-*p*-(dimethylaminophenyl))porphyrinato)cobalt(II) and *meso*-(tetrakis(pentafluorophenyl)porphyrinato)cobalt(II), the Co–N distances are somewhat longer, 1.971(6) and 1.976(5) Å, respectively.²¹ Also in $\text{Co}^{\text{II}}(\text{OEP})$, which is planar, the Co–N distances, 1.967(3) and 1.975(2) Å, are somewhat longer than they are in $\{(\text{OEOP})\text{Co}^{\text{II}}\}^+$.²²

The oxaporphyrin unit is ordered and planar. Unlike other oxaporphyrin structures which display orientational disorder that involves multiple sites for the *meso*-oxa group,^{6,23} this structure refined with only one site for the oxygen atom. Diagram A of Figure 4 shows the out-of-plane displacements of the oxaporphyrin core atoms in the cation. These displacements are all small, less than 0.07 Å.

In the solid state, individual complex cations interact in a face-to-face fashion. This is seen in Figure 5 which shows the packing of all of the constituents of the solid and in Figure 6 which shows two views of the same pair of cations. Face-to-

(17) Balch, A. L.; Mazzanti, M.; Olmstead, M. M. *J. Am. Chem. Soc.* **1994**, *116*, 9114.

(18) Bonnett, R.; Buckley, D. G.; Hamzesh, D. *J. Chem. Soc., Perkin Trans I* **1981**, 322.

(19) LaMar, G. N.; Walker, F. A. *J. Am. Chem. Soc.* **1973**, *95*, 1790.

(20) Madura, P.; Scheidt, W. R. *Inorg. Chem.* **1976**, *15*, 3182.

(21) Kadish, K. M.; Araullo-McAdams, C.; Han, B. C.; Franzen, M. M. *J. Am. Chem. Soc.* **1990**, *112*, 8364.

(22) Scheidt, W. R.; Turowska-Tyrk, I. *Inorg. Chem.* **1994**, *33*, 1314.

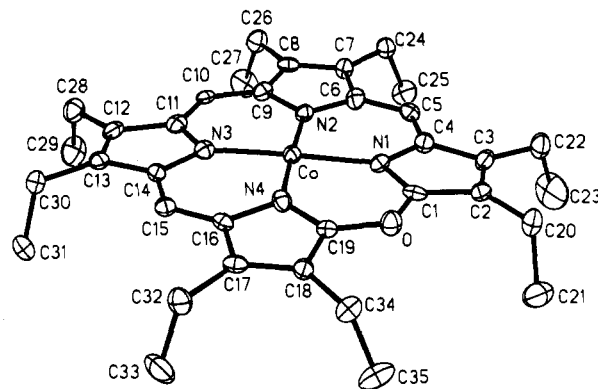
(23) Balch, A. L.; Noll, B. C.; Safari, N. *Inorg. Chem.* **1993**, *32*, 2901.

Table 1. Atomic Coordinates ($\times 10^4$) and Equivalent Isotropic Displacement Coefficients ($\text{\AA}^2 \times 10^3$) for $[(\text{OEP})\text{Co}^{\text{II}}](\text{PF}_6)\cdot\text{CH}_2\text{Cl}_2$

atom	x	y	z	$U(\text{eq})^a$
Co	943(1)	3(1)	4149(1)	16(1)
O	324(4)	2214(3)	4468(3)	24(2)
N(1)	-189(5)	466(3)	3304(3)	16(2)
N(2)	328(5)	-1347(3)	3003(3)	16(2)
N(3)	2147(4)	-402(4)	5009(3)	18(2)
N(4)	1550(5)	1379(4)	5263(3)	19(2)
C(1)	-316(6)	1406(4)	3546(4)	20(2)
C(2)	-1237(6)	1507(5)	2747(4)	20(3)
C(3)	-1705(6)	565(5)	1943(4)	22(3)
C(4)	-1069(6)	-89(5)	2271(4)	21(3)
C(5)	-1254(6)	-1102(4)	1710(4)	21(3)
C(6)	-614(6)	-1698(5)	2037(4)	21(3)
C(7)	-846(6)	-2783(4)	1417(4)	20(3)
C(8)	-24(6)	-3080(4)	2014(4)	18(2)
C(9)	702(6)	-2193(4)	2986(4)	20(3)
C(10)	1627(5)	-2172(4)	3805(4)	15(2)
C(11)	2331(6)	-1345(5)	4735(4)	19(3)
C(12)	3334(6)	-1337(4)	5573(4)	21(3)
C(13)	3765(6)	-381(5)	6364(4)	20(3)
C(14)	3024(6)	193(4)	6015(4)	18(3)
C(15)	3189(6)	1224(4)	6584(4)	19(3)
C(16)	2536(5)	1792(4)	6255(4)	16(2)
C(17)	2743(6)	2886(4)	6813(4)	19(3)
C(18)	1920(6)	3154(4)	6187(4)	18(3)
C(19)	1231(6)	2217(4)	5269(4)	18(3)
C(20)	-1535(6)	2481(5)	2858(5)	27(3)
C(21)	-445(7)	3414(5)	2709(5)	38(3)
C(22)	-2687(6)	228(5)	874(4)	29(3)
C(23)	-1983(8)	525(7)	118(5)	65(5)
C(24)	-1805(6)	-3421(5)	333(4)	23(3)
C(25)	-1170(7)	-3099(5)	-467(4)	35(3)
C(26)	185(6)	-4107(5)	1729(5)	27(3)
C(27)	1369(7)	-3983(5)	1319(5)	41(3)
C(28)	3807(6)	-2228(5)	5506(5)	29(3)
C(29)	4833(7)	-2169(6)	4929(5)	41(4)
C(30)	4847(6)	43(5)	7395(4)	25(3)
C(31)	6232(6)	792(5)	7406(5)	37(3)
C(32)	3761(6)	3587(5)	7872(4)	24(3)
C(33)	5176(6)	4210(5)	7854(5)	40(3)
C(34)	1720(6)	4171(5)	6360(5)	26(3)
C(35)	2478(7)	4915(5)	5843(5)	41(3)
Cl(1)	3428(3)	3660(2)	3642(2)	83(2)
Cl(2)	2481(3)	1408(2)	2437(2)	109(2)
C(36)	3531(9)	2758(7)	2613(6)	64(5)
P	4242(2)	7055(1)	9456(1)	32(1)
F(1)	4504(9)	8135(6)	9168(7)	40(3)
F(2)	4571(12)	7668(8)	10661(6)	58(4)
F(3)	3836(11)	6381(9)	8244(6)	56(4)
F(4)	3853(13)	5941(6)	9668(6)	49(3)
F(5)	5741(9)	7263(9)	9598(8)	60(4)
F(6)	2675(8)	6888(9)	9324(8)	61(3)
F(1A)	4234(11)	8175(6)	9428(9)	43(3)
F(2A)	4921(12)	7652(8)	10688(6)	38(3)
F(3A)	3714(12)	6558(10)	8238(7)	52(5)
F(4A)	4430(14)	5990(6)	9568(7)	45(3)
F(5A)	5858(9)	7502(9)	9450(8)	43(3)
F(6A)	2764(10)	6577(11)	9457(9)	76(5)

^a Equivalent isotropic U defined as one-third of the trace of the orthogonalized U_{ij} tensor.

face contacts within porphyrin complexes are a common feature of their solid state structures and these contacts have been carefully analyzed.²⁴ The interaction seen for $[(\text{OEP})\text{Co}^{\text{II}}]^+$ places this ion in the class of porphyrin dimers where the interaction is viewed as strong. Within the dimeric unit shown in Figure 5 the $\text{Co}\cdots\text{Co}$ distance is 3.487 Å and the $\text{Co}-\text{N}(4')$ distance is 3.166 Å. The lateral shift, as described in ref 24, is 1.506 Å and the mean-plane separation is 3.261 Å. The orientation of the two components within this cation pair resembles

**Figure 3.** Perspective view of the cation in $[(\text{OEP})\text{Co}^{\text{II}}](\text{PF}_6)$ with 50% thermal contours for all atoms.**Table 2.** Selected Bond Lengths and Angles for $[(\text{OEP})\text{Co}^{\text{II}}](\text{PF}_6)\cdot\text{CH}_2\text{Cl}_2$

Bond Lengths (Å)			
Co-N(1)	1.943(6)	C(3)-C(4)	1.447(11)
Co-N(2)	1.940(4)	C(4)-C(5)	1.360(9)
Co-N(3)	1.949(6)	C(5)-C(6)	1.376(11)
Co-N(4)	1.944(4)	C(6)-C(7)	1.454(9)
O-C(1)	1.340(6)	C(7)-C(8)	1.358(10)
O-C(19)	1.348(8)	C(8)-C(9)	1.436(7)
N(1)-C(1)	1.341(9)	C(9)-C(10)	1.366(9)
N(1)-C(4)	1.412(6)	C(10)-C(11)	1.362(6)
N(2)-C(6)	1.382(7)	C(11)-C(12)	1.444(9)
N(2)-C(9)	1.384(9)	C(12)-C(13)	1.360(8)
N(3)-C(11)	1.381(9)	C(13)-C(14)	1.438(10)
N(3)-C(14)	1.387(6)	C(14)-C(15)	1.393(9)
N(4)-C(16)	1.417(7)	C(15)-C(16)	1.353(10)
N(4)-C(19)	1.341(9)	C(16)-C(17)	1.450(8)
C(1)-C(2)	1.431(9)	C(17)-C(18)	1.354(10)
C(2)-C(3)	1.350(8)	C(18)-C(19)	1.422(7)

Bond Angles			
N(1)-Co-N(2)	90.2(2)	C(3)-C(4)-C(5)	127.5(5)
N(1)-Co-N(3)	177.5(2)	C(4)-C(5)-C(6)	126.2(5)
N(2)-Co-N(3)	91.3(2)	N(2)-C(6)-C(5)	124.5(5)
N(1)-Co-N(4)	88.1(2)	N(2)-C(6)-C(7)	110.9(6)
N(2)-Co-N(4)	178.1(2)	C(5)-C(6)-C(7)	124.6(5)
N(3)-Co-N(4)	90.4(2)	C(6)-C(7)-C(8)	106.2(5)
C(1)-O-C(19)	124.8(5)	C(7)-C(8)-C(9)	107.2(6)
Co-N(1)-C(1)	128.9(3)	N(2)-C(9)-C(8)	111.1(5)
Co-N(1)-C(4)	129.0(4)	N(2)-C(9)-C(10)	123.3(5)
C(1)-N(1)-C(4)	102.1(5)	C(8)-C(9)-C(10)	125.5(6)
Co-N(2)-C(6)	127.9(5)	C(9)-C(10)-C(11)	126.9(6)
Co-N(2)-C(9)	127.5(4)	N(3)-C(11)-C(10)	123.9(6)
C(6)-N(2)-C(9)	104.6(4)	N(3)-C(11)-C(12)	110.7(4)
Co-N(3)-C(11)	127.0(3)	C(10)-C(11)-C(12)	125.4(6)
Co-N(3)-C(14)	128.1(4)	C(11)-C(12)-C(13)	106.8(6)
C(11)-N(3)-C(14)	104.8(5)	C(12)-C(13)-C(14)	106.8(5)
Co-N(4)-C(16)	128.6(5)	N(3)-C(14)-C(13)	110.8(5)
Co-N(4)-C(19)	129.3(4)	N(3)-C(14)-C(15)	123.9(6)
C(16)-N(4)-C(19)	101.9(4)	C(13)-C(14)-C(15)	125.2(5)
O-C(1)-N(1)	124.8(6)	C(14)-C(15)-C(16)	126.0(5)
O-C(1)-C(2)	119.6(6)	N(4)-C(16)-C(15)	122.9(5)
N(1)-C(1)-C(2)	115.6(4)	N(4)-C(16)-C(17)	110.1(6)
C(1)-C(2)-C(3)	104.4(6)	C(15)-C(16)-C(17)	127.0(5)
C(1)-C(2)-C(20)	124.2(5)	C(16)-C(17)-C(18)	107.5(4)
C(3)-C(2)-C(20)	131.4(6)	C(17)-C(18)-C(19)	104.3(6)
C(2)-C(3)-C(4)	107.5(5)	O-C(19)-N(4)	124.1(4)
N(1)-C(4)-C(3)	110.4(5)	O-C(19)-C(18)	119.8(6)
N(1)-C(4)-C(5)	122.1(6)	N(4)-C(19)-C(18)	116.1(5)
C(2)-C(20)-C(21)	113.0(6)		

the orientation of cations in $[(\text{OEP})\text{Fe}^{\text{III}}(2\text{-MeHIm})]^+$ ²⁵ and in $[(\text{OEP})\text{FeNO}]^+$.²⁶ Note that the second axial site on cobalt is

(25) Scheidt, W. R.; Geiger, D. K.; Lee, Y. J.; Reed, C. A.; Lang, G. J. *Am. Chem. Soc.* **1985**, *107*, 5693.

(26) Scheidt, W. R.; Lee, Y. J.; Hatano, K. *J. Am. Chem. Soc.* **1984**, *106*, 3191.

(24) Scheidt, W. R.; Lee, J. Y. *Struct. Bonding* **1987**, *64*, 1.

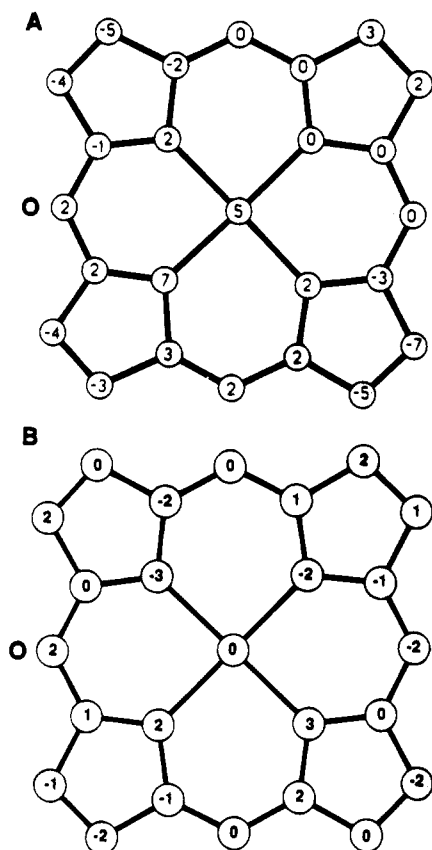


Figure 4. Diagrams of the oxaporphyrin cores of A, $[(\text{OEP})\text{Co}^{\text{II}}]^+$, and B, $\{(\text{OEP})\text{Co}^{\text{III}}\text{Cl}_2\}$, in which the out-of-plane displacements (in units of 0.01 Å) are shown for each atom.

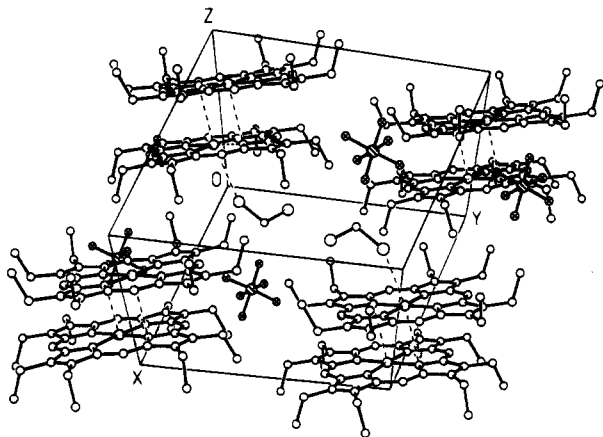


Figure 5. View of the packing of all constituents within $[(\text{OEP})\text{Co}^{\text{II}}](\text{PF}_6)$. Only one orientation of the hexafluorophosphate ion is shown.

blocked by a chlorine atom of the dichloromethane molecule with a nonbonded $\text{Co} \cdots \text{Cl}$ distance of 3.782 Å.

Crystal and Molecular Structure of $\{(\text{OEP})\text{Co}^{\text{III}}\text{Cl}_2\} \cdot 2\text{CH}_2\text{Cl}_2$. This complex has also been examined by X-ray crystallography. Atomic positional parameters are given in Table 3. Selected interatomic distances and angles are set out in Table 4.

A view of the complex is shown in Figure 7. The cobalt ion is located at an inversion center. There is disorder in the location of the oxa bridge which is equally distributed between the site specified in Figure 7 and at the site labeled C(6'). Such disorder has been seen with other oxaporphyrin complexes.^{6,23}

The cobalt ion is six-coordinate with two axial chloride ligands. The $\text{Co}-\text{N}$ distances (1.964(5), 1.956(5) Å) fall in

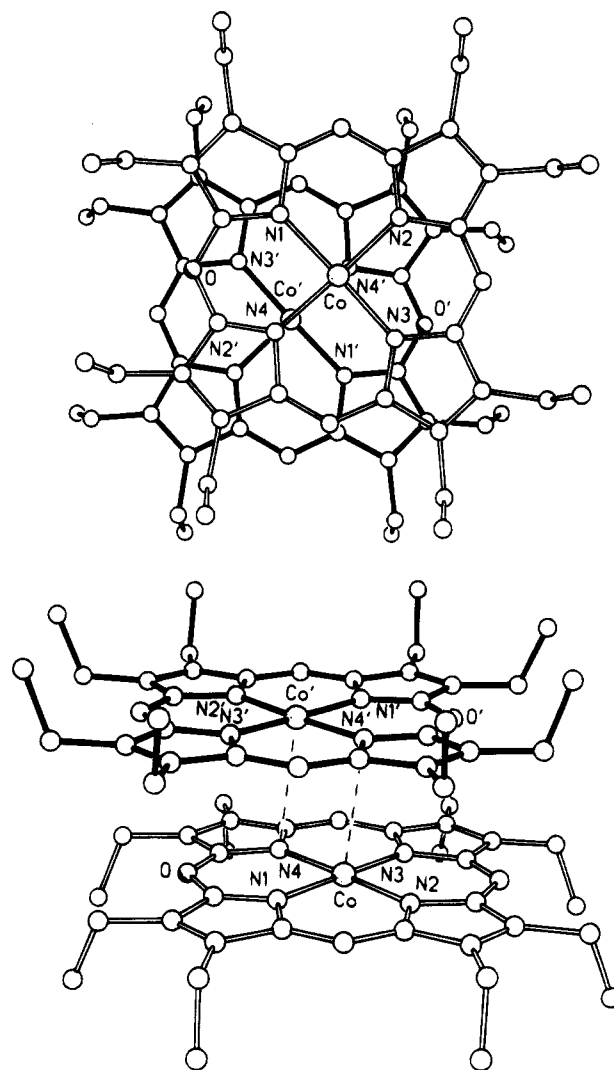


Figure 6. Two views that show the close approach of pairs of cations within the solid state structure of $[(\text{OEP})\text{Co}^{\text{II}}](\text{PF}_6)$.

the range seen for cobalt(III) porphyrin complexes.²⁷ The $\text{Co}-\text{Cl}(1)$ distance 2.253(2) Å is near the range of distances (2.149–2.251 Å) for other cobalt(III) porphyrin complexes with axial chloride ligands.^{28–30}

The oxaporphyrin ring is planar. The out-of-plane displacements of the atoms within the core of the macrocycle are shown in diagram B of Figure 4 where they are readily compared with those of $[(\text{OEP})\text{Co}^{\text{II}}]^+$. The oxaporphyrin in the cobalt(III) complex is even more nearly planar than that in the cobalt(II) complex.

Discussion

The synthetic work described here shows that the coupled oxidation process that has been studied for some time with iron porphyrins in pyridine solution can also occur with a cobalt porphyrin, but a different solvent system is required. In pyridine solution treatment of $\{(\text{OEP})\text{Co}^{\text{II}}\}$ with ascorbic acid and dioxygen merely results in the oxidation to cobalt(III), and

(27) Arasasingham, R. D.; Balch, A. L.; Olmstead, M. M.; Renner, M. W. *Inorg. Chem.* **1987**, *26*, 3562.

(28) Sakurai, T.; Yamamoto, K.; Seino, N.; Katsuta, T. *Acta Crystallogr.* **1975**, *31B*, 2514.

(29) Sakurai, T.; Yamamoto, K.; Naito, H.; Nakamoto, N. *Bull. Chem. Soc. Jpn.* **1976**, *49*, 3042.

(30) Iimura, Y.; Sakurai, T.; Yamamoto, K. *Bull. Chem. Soc. Jpn.* **1988**, *61*, 821.

Table 3. Atomic Coordinates ($\times 10^4$) and Equivalent Isotropic Displacement Coefficients ($\text{\AA}^2 \times 10^3$) for $\{(\text{OEP})\text{Co}^{\text{III}}\text{Cl}_2\} \cdot 2\text{CH}_2\text{Cl}_2$

atom	x	y	z	$U(\text{eq})^a$
Co	5000	5000	5000	24(1)
Cl(1)	5947(1)	3725(2)	5958(1)	30(1)
N(1)	5619(4)	3471(7)	4400(2)	23(2)
N(2)	6187(4)	6532(7)	4996(2)	24(2)
C(1)	4331(5)	1237(8)	4307(3)	24(2)
C(2)	5246(5)	1948(8)	4162(3)	24(2)
C(3)	5957(5)	1180(9)	3753(3)	25(2)
C(4)	6774(5)	2246(8)	3757(3)	24(2)
C(5)	6543(5)	3644(9)	4158(3)	26(2)
C(6)	7187(4)	4981(8)	4285(2)	32(1)
O	7187(4)	4981(8)	4285(2)	32(1)
C(7)	7031(5)	6340(9)	4665(3)	26(2)
C(8)	7740(5)	7743(9)	4758(3)	30(2)
C(9)	7312(5)	8819(9)	5154(3)	28(2)
C(10)	6339(5)	8073(8)	5295(3)	27(2)
C(11)	5766(5)	-454(8)	3383(3)	34(3)
C(12)	5087(6)	-289(9)	2645(3)	47(3)
C(13)	7758(5)	2065(9)	3436(3)	36(3)
C(14)	7678(5)	2949(10)	2729(3)	42(3)
C(15)	8756(5)	7857(10)	4471(3)	43(3)
C(16)	9717(5)	7263(10)	4981(4)	55(3)
C(17)	7721(5)	10485(8)	5399(3)	32(2)
C(18)	8433(6)	10490(9)	6133(3)	45(3)
Cl(2)	7966(3)	7937(3)	2375(1)	95(1)
Cl(3)	9581(2)	9902(4)	1875(2)	97(1)
C(19)	8303(6)	9045(11)	1670(4)	63(3)

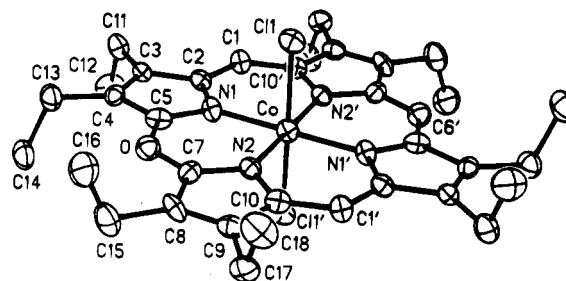
^a Equivalent isotropic U defined as one-third of the trace of the orthogonalized U_{ij} tensor.

Table 4. Bond Lengths and Angles for $\{(\text{OEP})\text{Co}^{\text{III}}\text{Cl}_2\} \cdot 2\text{CH}_2\text{Cl}_2$

Bond Lengths (\AA)			
Co-Cl(1)	2.253(2)	C(2)-C(3)	1.452(9)
Co-N(1)	1.964(5)	C(3)-C(4)	1.351(9)
Co-N(2)	1.956(5)	C(4)-C(5)	1.436(9)
N(1)-C(2)	1.372(8)	C(5)-C(6),[O]	1.354(9)
N(1)-C(5)	1.353(8)	C(6),[O]-C(7)	1.361(9)
N(2)-C(7)	1.360(8)	C(7)-C(8)	1.443(10)
N(2)-C(10)	1.377(8)	C(8)-C(9)	1.346(10)
C(1)-C(2)	1.375(9)	C(9)-C(10)	1.449(9)
C(1)-C(10)	1.373(9)		
Bond Angles (deg)			
Cl(1)-Co-N(1)	89.0(1)	C(3)-C(4)-C(5)	105.8(6)
Cl(1)-Co-N(2)	90.4(1)	N(1)-C(5)-C(4)	112.8(6)
N(1)-Co-N(2)	90.2(2)	N(1)-C(5)-C(6)	123.7(6)
Co-N(1)-C(2)	128.1(4)	C(4)-C(5)-C(6),[O]	123.5(6)
Co-N(1)-C(5)	127.8(4)	N(1)-C(5)-C(6),[O]	123.7(6)
C(2)-N(1)-C(5)	104.0(5)	C(5)-C(6),[O]-C(7)	127.0(5)
Co-N(2)-C(7)	127.4(4)	N(2)-C(7)-C(6),[O]	123.9(6)
Co-N(2)-C(10)	128.5(4)	N(2)-C(7)-C(8)	112.4(6)
C(7)-N(2)-C(10)	104.1(5)	C(6),[O]-C(7)-C(8)	123.7(6)
C(2)-C(1)-C(10)	125.7(6)	C(7)-C(8)-C(9)	105.8(6)
N(1)-C(2)-C(1)	124.1(6)	C(8)-C(9)-C(10)	106.8(6)
N(1)-C(2)-C(3)	111.1(5)	N(2)-C(10)-C(9)	110.9(6)
C(1)-C(2)-C(3)	124.8(6)	N(2)-C(10)-C(1)	123.7(6)
C(2)-C(3)-C(4)	106.2(6)	C(9)-C(10)-C(1)	125.3(6)

^a Symmetry code: prime denotes $1 - x, 1 - y, 1 - z$.

ascorbic acid is insufficient at re-reduction to the cobalt(II) state.¹⁴⁻¹⁶ As Scheme 1 shows, a variety of products can be obtained from the coupled oxidation of $\{(\text{OEP})\text{Co}^{\text{II}}\}$ when the reaction is run in the poorly coordinating solvent mixture of dichloromethane and tetrahydrofuran. For this reaction to be successful it is important that both solvent components be present. Tetrahydrofuran is used to give sufficient solubility of the ascorbic acid, but with tetrahydrofuran alone as solvent, over-oxidation results in bleaching of the color of the porphyrin-derived products. Dichloromethane is involved directly in the reaction that results in the formation of $\{(\text{OEP})\text{Co}^{\text{III}}\text{Cl}_2\}$, since the solvent is the only source of the chloro ligands. Cooling

**Figure 7.** Perspective view of $\{(\text{OEP})\text{Co}^{\text{III}}\text{Cl}_2\}$ with 50% thermal contours for all atoms.

of the anaerobically prepared solution of the reactants in a liquid nitrogen bath prior to the addition of dioxygen is also necessary to ensure good yields. This process apparently facilitates the reaction by increasing the concentration of dioxygen in the mixture. The products obtained in this process are similar to those obtained from coupled oxidation of $\{(\text{OEP})\text{Fe}^{\text{II}}(\text{py})_2\}$ in that complexes of both octaethylporphyrin⁶ and octaethylbilindione⁷ are present. Despite the similarities of the cobalt and iron based chemistry, there still is no assurance that the formation of a metal-bound dioxygen ligand is an essential participant in the porphyrin degradation. It is just as likely that an essential feature for success of the coupled oxidation process is the redox potential of the $\text{Fe}^{\text{II}}/\text{Fe}^{\text{III}}$ or the $\text{Co}^{\text{II}}/\text{Co}^{\text{III}}$ couple and that these potentials are modulated by the ability of the solvent to act as an axial ligand. Further work aimed at identifying the reactive forms of dioxygen that participate in these reactions are in progress.

Experimental Section

Preparation of Compounds. H_2OEP was purchased from Aldrich and cobalt(II) was inserted by a standard procedure.³¹

Oxygenation of $\{(\text{OEP})\text{Co}^{\text{II}}\}$. A 100 mg (0.169 mmol) sample of $\{(\text{OEP})\text{Co}^{\text{II}}\}$ was added to a dioxygen-free suspension of 400 mg (2.27 mmol) of ascorbic acid in a mixture of 80 mL of dichloromethane and 10 mL of tetrahydrofuran. The sample was cooled in a liquid nitrogen bath until it partly froze. Dioxygen was vigorously bubbled through the slurry. The mixture was stirred and allowed to warm to room temperature under an atmosphere of dioxygen. The mixture, which initially was red, became green after 2 h of stirring under a dioxygen atmosphere. This green suspension was used to form various products as described below.

$\{(\text{OEP})\text{Co}^{\text{III}}\text{Cl}_2\}$. The green suspension was evaporated to dryness. The solid was extracted with 80 mL of dichloromethane, filtered to remove excess ascorbic acid, and then stirred in air for 24 h. The volume of the green solution was reduced to 5 mL. This solution was subjected to chromatography on a 2.5 by 15 cm column of silica gel. Elution of the column with dichloromethane produced an initial pink band that contained unreacted $\{(\text{OEP})\text{Co}^{\text{II}}\}$. The second, red-green band was collected and evaporated to dryness to give a burgundy-red microcrystalline solid (70 mg, 62%). The product could be recrystallized by dissolution in dichloromethane and reprecipitation through the slow addition of *n*-hexane. The electronic absorption spectrum is shown in Figure 1. ¹H NMR (300 MHz, chloroform-*d*): δ = 9.71 (2), 9.70 (1) (meso-H), 3.68 (16) (multiplet, methylene-H); 1.85, 1.83, 1.82, 1.79 (24) overlapping triplets, methyl-H). Dark red needles of $\{(\text{OEP})\text{Co}^{\text{III}}\text{Cl}_2\} \cdot 2\text{CH}_2\text{Cl}_2$ that were suitable for X-ray crystallography were obtained by diffusion of a layer of *n*-hexane into a dichloromethane solution of the complex.

$\{(\text{OEP})\text{Co}^{\text{II}}(\text{PF}_6)_2\}$. The green suspension was filtered to remove the ascorbic acid and then the sample was evaporated to dryness. Under a dinitrogen atmosphere, the solid was dissolved in 5 mL of dichloromethane and subjected to chromatography on a silica gel column (2.5 \times 15 cm). Elution with dichloromethane produced an initial pink

(31) Adler, A. D.; Longo, F. R.; Kampas, F.; Kim, J. J. *Inorg. Nucl. Chem.* 1970, 32, 2443.

band that contained unreacted $\{(\text{OEP})\text{Co}^{\text{II}}\}$ and a red-green band that was collected and evaporated to dryness to give 23 mg (21% yield) of $\{(\text{OEP})\text{Co}^{\text{III}}\text{Cl}_2\}$. Further elution with a 1:10 v/v mixture of tetrahydrofuran and dichloromethane produced a red band which was not identified. Finally elution with methanol produced a blue band that was collected and evaporated to dryness. This solid was dissolved in 30 mL of dioxygen-free methanol, and 0.8 g of ammonium hexafluorophosphate was added. The resulting suspension was evaporated to dryness. The solid was dissolved under an inert atmosphere in 30 mL of dioxygen-free dichloromethane. The suspension was filtered, evaporated to 10 mL, and treated with 20 mL of *n*-hexane. The purple, microcrystalline solid, which dissolves to give blue solutions, was collected by filtration and washed with *n*-hexane to yield 60 mg (48%) of the product. The electronic absorption spectrum is given in Figure 1 and the ^1H NMR spectrum in Figure 2. Dark red blocks of $\{(\text{OEP})\text{Co}^{\text{II}}\}(\text{PF}_6)\text{CH}_2\text{Cl}_2$ that were suitable for X-ray crystallography were obtained by diffusion of dioxygen-free *n*-hexane into a dioxygen-free, dichloromethane solution of the complex.

$\{(\text{OEB})\text{Co}\}$. The green suspension was stirred in air for an additional hour. The suspension was then filtered to remove the excess ascorbic acid. The filtrate was washed with two 100-mL portions of water. The organic solution was then evaporated to dryness. The solid residue was dissolved in 5 mL of dichloromethane and subjected to chromatography on silica gel column (2.5 × 15 cm). Elution with dichloromethane produced an initial pink band that contained unreacted $\{(\text{OEP})\text{Co}^{\text{II}}\}$. The second green band was collected and evaporated to dryness to yield $\{(\text{OEB})\text{Co}\}$ as a microcrystalline olive-green solid; yield 25 mg, 24%. The electronic absorption spectrum is given in Figure 1. ^1H NMR (300 MHz, dichloromethane- d_2 , 24°C): δ = 11.90 (1) (s), 5.96 (2) (s, meso-H), 4.61 (2), 4.07 (2), 3.75 (2), 3.03 (2), 2.52 (2), 2.30 (2) (sextets), 2.20 (4) (multiplet, methylene-H), 1.97 (6), 1.74 (6), 1.31 (6), 1.23 (6) (triplets, methyl-H).

H_3OEB . The green suspension was filtered to remove excess ascorbic acid. The filtrate was washed with two 100-mL portions of water, and the organic solution was then evaporated to dryness. The residue was dissolved in 5 mL of acetone. A solution of 12 mg of sodium hydroxide in 5 mL of methanol was added. The resulting reddish solution was stirred for 1 h under a dinitrogen atmosphere; 3 mL of a 0.1 M solution of dioxygen free hydrochloric acid was added. The solution was stirred for 12 h. The purple solution was evaporated to dryness under vacuum. The solvent was again evaporated. The residue was dissolved in 5 mL of dichloromethane, washed with 100 mL of water and dried over sodium sulfate. The solution was then subjected to chromatography on a 2.5 × 18 cm column of silica gel. Elution with dichloromethane produced a pink band of $\{(\text{OEP})\text{Co}^{\text{II}}\}$. Further elution with 10% tetrahydrofuran in dichloromethane produced a purple band which was set aside and a blue band which was collected and evaporated to give H_3OEB as a blue, microcrystalline solid yield; 47 mg, 50%.

Instrumentation. ^1H NMR spectra were recorded on a General Electric QE-300 FT spectrometer operating in the quadrature mode (^1H frequency is 300 MHz). The spectra were collected over a 50-kHz bandwidth with 16K data points and a 10- μs 90° pulse. For a typical spectrum, between 1000 and 5000 transients were accumulated with a 50-ms delay time. The signal-to-noise ratio was improved by apodization of the free induction decay. The residual ^1H spectrum of CDCl_3 or CD_2Cl_2 was used as a secondary reference. To obtain unambiguous methyl assignments in the diamagnetic region of T_1 values, an inversion recovery sequence was used with τ values varying between 0.2 and 100 ms.³² Magnetic moments from solutions were obtained by the Evans method.³³ In the solid state, magnetic moment measurements were made with a Quantum Design SQUID magnetometer.

X-ray Data Collection. A crystal of $\{(\text{OEP})\text{Co}^{\text{II}}\}(\text{PF}_6)\text{CH}_2\text{Cl}_2$ was coated with a light hydrocarbon oil and mounted in the 130 K dinitrogen

Table 5. Crystal Structure Data

	$\{(\text{OEP})\text{Co}^{\text{II}}\}(\text{PF}_6)\text{CH}_2\text{Cl}_2$	$\{(\text{OEP})\text{Co}^{\text{III}}\text{Cl}_2\}\cdot 2\text{CH}_2\text{Cl}_2$
formula	$\text{C}_{36}\text{H}_{45}\text{Cl}_2\text{CoF}_6\text{N}_4\text{OP}$	$\text{C}_{37}\text{H}_{47}\text{Cl}_6\text{CoN}_4\text{O}$
fw	824.6	835.4
cryst syst	triclinic	monoclinic
space group	$P\bar{1}$	$P2_1/c$
<i>a</i> , Å	11.077(2)	12.702(5)
<i>b</i> , Å	14.033(2)	8.125(3)
<i>c</i> , Å	14.099(3)	19.327(5)
α , deg	104.56(2)	90
β , deg	101.70(2)	101.23(2)
γ , deg	110.70(1)	90
<i>V</i> , Å ³	1878.7(6)	1956.4(11)
<i>Z</i>	2	
<i>T</i> , K	130	130
λ (Mo K α)	0.710 73	0.710 73
μ , mm ⁻¹	0.707	0.884
d_{calc} , Mg/M ³	1.458	1.418
transm	0.87–0.92	0.92–0.94
factors		
R^a	0.066	0.057
R_w^b	0.060 ^c	0.054 ^d

$$^a R = \sum ||F_o| - |F_c||/|F_o|. \quad ^b R_w = \sum ||F_o| - |F_c||w^{1/2}/\sum |F_o|w^{1/2}. \quad ^c w^{-1} = \sigma^2(F) + 0.0003F^2. \quad ^d w^{-1} = \sigma^2(F) + 0.0005F^2.$$

stream of a Syntex P2₁ diffractometer that was equipped with a locally modified LT-1 low temperature apparatus. A crystal of $\{(\text{OEP})\text{Co}^{\text{III}}\text{Cl}_2\}$ was similarly coated with a hydrocarbon oil and mounted in the 130 K dinitrogen stream of a Siemens R3m/V diffractometer that was equipped with an Enraf-Nonius low temperature device. Intensity data were collected through the use of graphite monochromated MoK α (λ = 0.71073 Å) radiation. Crystal data for both compounds are given in Table 5. Check reflections showed only random (<2%) variation during data collection. The data were corrected for Lorentz and polarization effects. Further details are given in the supplementary material.

Solution and Structure Refinement. Calculations were performed with the SHELXTL Plus series of programs. Scattering factors and corrections for anomalous dispersion were taken from a standard source.³⁴ Both structures were solved by direct methods. Absorption corrections were applied to both structures.³⁵ Hydrogen atoms were fixed to appropriate carbon atoms through the use of a riding model with a fixed, isotropic *U*. For $\{(\text{OEP})\text{Co}^{\text{II}}\}(\text{PF}_6)\text{CH}_2\text{Cl}_2$ two different orientations of the fluorine atoms about a common phosphorus atom were observed with occupancies of 0.54 and 0.46. Their relative orientations are shown in the supplementary material.

For $\{(\text{OEP})\text{Co}^{\text{III}}\text{Cl}_2\}\cdot 2\text{CH}_2\text{Cl}_2$, refinement was carried out with equal contributions from carbon and oxygen atoms at the meso sites, O and C(6'), but with the positional and thermal parameters tied together. The location of the oxygen atom at these two sites was clearly indicated by the magnitude of the thermal parameters.

Acknowledgment. We thank the National Institutes of Health (GM-26226) for financial support and Richard Koerner and Dr. P. Klavins for valuable experimental assistance.

Supplementary Material Available: Tables of crystal data, data collection, structure solution and refinement, bond distances, bond angles, and anisotropic thermal parameters for $\{(\text{OEP})\text{Co}^{\text{II}}\}(\text{PF}_6)\text{CH}_2\text{Cl}_2$ and $\{(\text{OEP})\text{Co}^{\text{III}}\text{Cl}_2\}\cdot 2\text{CH}_2\text{Cl}_2$ and a diagram of the PF_6^- anion in $\{(\text{OEP})\text{Co}^{\text{II}}\}(\text{PF}_6)\text{CH}_2\text{Cl}_2$ (18 pages). Ordering information is given on any current masthead page.

IC941271B

(32) Inubushi, T.; Becker, E. D. *J. Magn. Reson.* **1983**, *51*, 128.(33) Evans, D. F. *J. Chem. Soc.* **1959**, 2003.(34) *International Tables for X-ray Crystallography*, D. Reidel Publishing Co.; Boston, MA, 1992; Vol. C.

(35) Moezzi, B. Ph.D. Thesis, University of California, Davis, CA, 1987.